Surface plasmon-polariton mediated light emission through thin metal films

Stephen Wedge and W. L. Barnes

Thin Films Photonics Group, School of Physics, Stocker Road, University of Exeter, Exeter, EX4 4QL, UK
s.wedge@exeter.ac.uk

Abstract: The emission of light by sources in close proximity to a thin metallic film is dominated by surface plasmon-polariton modes supported by that film. We explore the nature of the modes and examine how the energy lost to such modes can be recovered. Both cross-coupled and coupled SPPs are presented as a means of transferring energy across a thin metal film. These modes are then scattered and thereby coupled to light by a wavelength scale grating type microstructure. We show that the photoluminescence emission from a structure containing a microstructured thin metal film that supports coupled SPPs is over 50 times greater than that from a similar planar structure. Similar strong photoluminescence emission is also exhibited by a sample that contains a planar metal film coated with a microstructured dielectric overlayer.

OCIS codes: (230.3670) Light-emitting diodes; (240.6680) Surface plasmons.

References and links

1. L. H. Smith, J. A. E. Wasey, and W. L. Barnes, "The light out-coupling efficiency of top emitting organic light-emitting diodes," Appl. Phys. Lett. **84**, 2986-2988 (2004).
2. R. Windisch, S. Schoberth, S. Meinischmidt, P. Kiesel, A. Knobloch, P. Heremans, B. Dutta, G. Borghs, and G. H. Dohler, "Light propagation through textured surfaces," J. Mod. Opt. **1,** 512-516 (1999)
3. J. M. Lupton, B. J. Matterson, I. D. W. Samuel, M. J. Jory, and W. L. Barnes, "Bragg scattering from periodically microstructured light emitting diodes," Appl. Phys. Lett. **77**, 3340-3342 (2000).
4. P. A. Hobson, S. Wedge, J. A. E. Wasey, I. Sage and W.L. Barnes, "Surface plasmon mediated emission from organic light-emitting diodes," Adv. Mater. **14**, 1393-1396 (2002).
5. W. L. Barnes, "Electromagnetic crystals for surface plasmon polaritons and the extraction of light from emissive devices," J. Lightwave Technol. **17**, 2170-2182 (1999)
6. W. L. Barnes, "Fluorescence near interfaces: the role of photonic mode density," J. Mod Opt. **45**, 661 – 699 (1998)
7. N. E. Hecker, R. A. Hopfel, N. Sawaki, T. Maier, and G. Strasser, "Surface plasmon enhanced photoluminescence from a single quantum well," Appl. Phys. Lett. **75**, 1577-1579 (1999).
8. A. Köck, E. Gornik, M. Hauser, and K. Beinstingl, "Strongly directional emission from AlGaAs/GaAs light emitting diodes," Appl. Phys. Lett. **57**, 2327-2329 (1990).
9. I. R. Hooper, J. R. Sambles, "Surface plasmon-polariton on thin-slab metal gratings," Phys. Rev. B **67**, 2354041-2354046 (2003).
10. T. W. Ebbesen, H. J. Lezec, H. F. Ghaemi, T. Thio, and P. A. Wolff, "Extraordinary optical transmission through sub-wavelength hole arrays," Nature, **391**, 667-669 (1998).
11. N. Bonod, S. Enoch, L. Li, E. Popov, and M. Nevière, "Resonant optical transmission through thin metallic films with and without holes," Opt. Express **11**, 482-490 (2003), http://www.opticsexpress.org/abstract.cfm?URI=OPEX-11-5-482.
12. R. W. Gruhlke, W. R. Holland, and D. G. Hall, "Surface-plasmon cross coupling in molecular fluorescence near a corrugated thin metal film," Phys. Rev. Lett. **56**, 2838-2841 (1986).
13. D. K. Gifford and D. G. Hall, "Extraordinary transmission of organic photoluminescence through an otherwise opaque metal layer via surface plasmon cross coupling," Appl. Phys. Lett. **80**, 3679-3681 (2002)
14. R. W. Gruhlke, W. R. Holland, and D. G. Hall, "Optical emission from coupled surface plasmons," Opt. Lett. **12**, 364-366 (1987)
15. R. M. Amos and W. L. Barnes, "Modification of the spontaneous emission rate of Eu^{3+} ions close to a thin metal mirror," Phys. Rev. B **55**, 7249-7254 (1997)
16. S. Wedge, I. R. Hooper, I. Sage and W. L. Barnes, "Light emission through a corrugated metal film: the role of cross-coupled surface plasmon-polaritons," Phys. Rev. B (to be published) (2004)
17. D. Sarid, "Long-range surface-plasma waves on very thin metal films," Phys. Rev. Lett. **47**, 1927-1930 (1981).

#4590 - $15.00 US Received 10 June 2004; Revised 29 June 2004; accepted 30 June 2004

18. P. T. Worthing and W. L. Barnes, "Efficient coupling of surface plasmon-polaritons to radiation using a bi-grating," Appl. Phys. Lett. **79**, 3035-3037 (2001).
19. P. T. Worthing and W. L. Barnes, "Coupling efficiency of surface plasmon-polaritons to radiation using a corrugated surface angular dependence," J. Mod. Opt. **49**, 1453-1462 (2002).
20. J. R. Lawrence, P. Andrew, M. Buck, W. L. Barnes, G. A. Turnbull and I. D. W. Samuel, "Optical properties of a light-emitting polymer directly patterned by soft lithography," Appl. Phys. Lett. **81**, 1955-1957 (2002)

1. Introduction

Organic light-emitting diodes (OLEDs) continue to attract attention as light sources for a number of applications. In the context of displays, top-emitting OLEDs are of increasing interest because they may be fabricated directly on top of an opaque substrate, such as silicon, thereby allowing display elements and control electronics to be integrated. In top-emitting OLED emission takes place through the metallic cathode, typically 50 – 100 nm thick. Efficiency is a key issue and, as with substrate-emitting OLEDs, optical out-coupling remains the least developed aspect of efficiency. Excitons are generated by the injection of charge carriers and it is the radiative decay of these excitons that produces light. Unfortunately the probability that exciton decay will lead to an emitted photon is reduced by coupling of the exciton to bound optical modes, specifically waveguide and surface plasmon-polariton (SPP) modes supported by the structure. As we have recently shown [1], power lost to SPPs can account for up to 40% of the power that would otherwise have been radiated. The subject of the emission of light through a metal film, such as the cathode of a top-emitting OLED provides an application in which an understanding of the role of surface plasmon-polaritons is both topical and potentially commercially important. In particular it is interesting to explore whether some of the power lost to SPP modes can be recovered, thereby improving device efficiency – it is just such an exploration that is the subject of the present paper.

SPPs are trapped electromagnetic surface modes at the interface between a metal and a dielectric and are a combined oscillation of the electromagnetic field and the surface charges of the metal. SPPs have electromagnetic fields that decay exponentially into both the metal and dielectric media that bound the interface. On a planar surface their combined electromagnetic field/surface charge nature means that they are non-radiative in nature.

Figure 1(a) shows a schematic dispersion diagram, angular frequency, ω, vs. in-plane wavevector, $k_{//}$ for a thin planar metal film bounded on one side by an organic layer and on the other by air (here in-plane refers to the plane defined by the interfaces of the structure and, where it refers to emission, $k_{//}$ is also in the plane containing the emission direction). The shaded area in Fig. 1(a) is the air light-cone; it represents those combinations of frequency and in-plane wavevector applicable to freely propagating photons in the air half-space. From Fig. 1(a) it may be seen that for a given frequency the wavevectors of the SPP modes always lie beyond this light cone, illustrating the mode's non-radiative nature.

#4590 - $15.00 US Received 10 June 2004; Revised 29 June 2004; accepted 30 June 2004

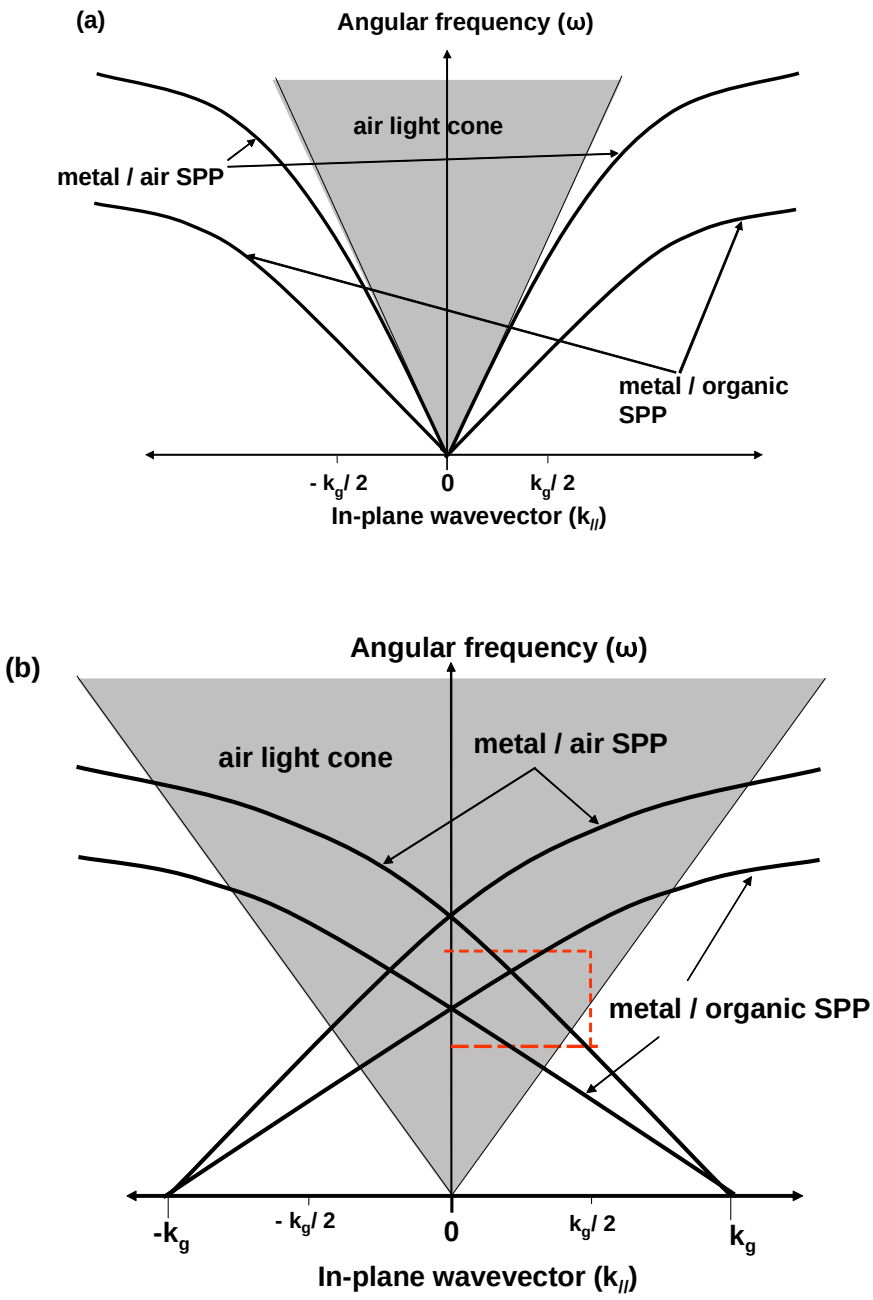

Fig. 1 (a). Schematic representation of a dispersion map for a thin metal film bordered on one side by an organic light-emitting material and on the other side by air. The shaded region labelled "air light-cone" represents the frequencies and wavevectors accessible to light propagating in air. Note, the in-plane wavevector range from $-k_g/2$ to $k_g/2$ corresponds to the first Brillouin zone. (b). A schematic representation of a dispersion map for a corrugated thin metal film bordered on one side by an organic light-emitting material and on the other side by air. The area enclosed within the dashed lines represents the range of frequencies and wavevectors presented in Figure 5. (Note that for clarity the horizontal scale used in Fig. 1(b) is not the same as Fig. 1(a.)

#4590 - $15.00 US
Received 10 June 2004; Revised 29 June 2004; accepted 30 June 2004

To recover the energy lost to SPP modes some means must be sought to reduce/augment the wavevectors of the SPPs so as to enable them to couple to light. A number of such methods have been used in the recovery of SPP modes, one approach has been the introduction of surface roughness to the metal thus allowing the SPPs to Bragg scatter to light [2]. Another approach to recover energy lost to bound SPP modes is to introduce wavelength scale microstructure into the device [3-5] thereby allowing trapped SPP modes to be Bragg scattered and thus couple to freely propagating radiation so as to produce emitted light. Here we use a microstructure in the form of a diffraction grating, in part because it allows us to gain insight into the nature of the SPP modes involved and the physics underlying the scattering process.

Figure 1(b) shows a schematic representation of the dispersion diagram of a microstructured thin metal film (pitch λ_g) bound on one side by an organic emissive material and on the other by air. The introduction of the microstructure allows the momentum (wavevector) of the SPPs to be augmented/reduced by Bragg scattering off the periodic structure according to the relation,

$$\boldsymbol{k}_{SPP} \pm n\boldsymbol{k}_g = \boldsymbol{k}_0 \sin\theta \qquad (1)$$

where $\boldsymbol{k}_{SPP}$ is the wavevector of the SPP mode, $\boldsymbol{k}_g$ is the grating wavevector($|\boldsymbol{k}_g| = 2\pi/\lambda_g$), $\boldsymbol{k}_0$ sin θ is in-plane wavevector, θ the polar angle of the emitted light and n is an integer that defines the order of the scattering process. The SPP modes may therefore be scattered into the light cone and thus couple to light.

As we show below, the recovery of energy lost to SPP modes is more complex than simply scattering these modes to produce emitted light. The excitons in an emissive material may couple to the SPP modes associated with each side of a thin metal film. Numerical calculations, modeling the emitter as an electric dipole (Fig. 2) show that this process is dominated by losses to the SPP mode associated with the metal/organic interface, with the coupling to this mode being approximately 2 orders of magnitude greater than that to the metal/air SPP [6]. The SPP mode associated with the metal/organic SPP may couple to light via one of two routes. Firstly it may be scattered by the microstructure at the metal/organic interface. The light will then be attenuated as it propagates through the metal before emerging into the far field. Secondly the microstructure at the metal/air boundary may scatter the mode. In this case it is the attenuated field associated with the metal/organic SPP that is scattered by the microstructure. Emission mediated via either of these two routes is attenuated to a similar degree on crossing the metal film. A key to explaining why this mode (SPP2) has often not been observed before [7-8] comes from recent work that shows that these two emission pathways are out of phase and thus destructively interfere [9]. Because of their similar amplitude there is almost complete cancellation, thus accounting for why this mode has not often been seen before in this context. In order to recover the energy lost to the SPP mode associated with metal/organic interface some means must be found to transfer this energy across the metal film and then scatter to light. Ideally we would like to, a) overcome the phase mismatch and, b) alleviate the attenuation through the metal film. The work reported below seeks to address both these issues.

#4590 - $15.00 US Received 10 June 2004; Revised 29 June 2004; accepted 30 June 2004

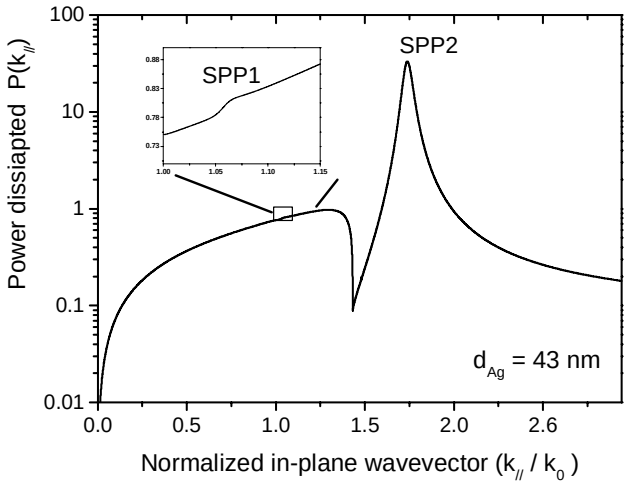

Fig. 2 Calculated power dissipation spectrum on a logarithmic scale for an emitter located in the light-emitting layer at a distance of 20 nm from the metal surface. The large peak at a normalized in-plane wavevector of ~ 1.7 represents power being lost to the metal/organic SPP (SPP2), the inset is an expanded plot (linear scale) of the feature associated with the metal/air SPP (SPP1).

The transfer of energy across a metal film has been the subject of much activity following the report of the enhanced transmission of light through metallic films perforated with periodic arrays of sub-wavelength holes by Ebbesen and co-workers [10]. As noted elsewhere [11] for the metal film thicknesses typical of top-emitting OLEDs holes are not needed, a periodic modulation will suffice. In this study we will focus on two methods for improving the coupling of energy associated with the SPP supported by the metal/organic interface (SPP2) across the metal film to produce light, firstly the use of cross-coupled SPPs and secondly the use of coupled SPPs.

The first method demonstrated as a means of transferring molecular fluorescence across a thin metal film was SPP cross-coupling [12-13]. SPP cross-coupling allows the mismatch in the in-plane wavevectors between the SPP modes associated with the interfaces on either side of a thin metal film to be overcome by the introduction to the metal of an appropriately scaled periodic microstructure. The SPPs may then couple when the follow condition is met,

$$\boldsymbol{k}_{SPP\,air} = \boldsymbol{k}_{SPP\,org} \pm n\boldsymbol{k}_{g} \qquad (2)$$

where, $\boldsymbol{k}_{SPPorg}$ and $\boldsymbol{k}_{SPPair}$ are the in-plane wavevectors of the SPPs associated with the metal/organic and metal/air interfaces respectively. The coupling between the SPP modes opens the possibility that the fields associated with the SPPs may span the metal at the frequency for which the cross-coupling condition, Eq. (2), is met enabling the transfer of energy across the metal. The metal/air SPP may then scatter to light by satisfying Eq. (1).

An alternative method of transferring energy across the metal film is the use of coupled SPPs [14]. Here the SPP modes associated with the two interfaces are coupled by matching the effective refractive indices of the materials bounding the metal thus allowing the fields associated with the SPPs to span the metal, across all emission frequencies. The SPP modes are then scattered to light, again by the introduction into the metal of a wavelength scale microstructure. Below we examine the photoluminescence emission of light through a thin metal film mediated by both cross-coupled and coupled SPP modes in greater detail and discuss the significance of these results on the efficiency of cathode emitting OLEDs is discussed.

#4590 - $15.00 US Received 10 June 2004; Revised 29 June 2004; accepted 30 June 2004

2. Sample fabrication

In order to investigate the role of cross-coupled and coupled SPPs in the emission of light through thin metal films, four different sample geometries were constructed. The first, used as a control sample, shown schematically in Fig. 3(a), consisted of a 60 nm thick emissive tris(8-hydroxyquinoline)aluminium (Alq_3) film deposited by thermal evaporation. The Alq_3 layer was coated with a 55 ± 2 nm thick planar silver film, again by thermal evaporation under vacuum (~10^{-7} Torr).

The second structure (Fig. 3(b)) was used to investigate the cross-coupling of SPPs as a means of energy transfer across the metal. This sample was similar in construction to the planar control structure (Fig. 3(a)) containing a 60 nm evaporated Alq_3 emissive layer and a 55 ± 2 nm Ag film however, the Ag film included a wavelength scale grating type microstructure (λ_g = 338 ± 1 nm). This microstructure was produced by spin coating the silica substrate with a ~ 300 nm thick photo-resist (Shipley Megaposit SPR 700-1.2) film and exposing this film to an interference pattern produced using a 325 nm He-Cd laser. The pattern was chemically developed and then transferred to the silica substrate by reactive-ion etching with a mixture of CHF_3 and O_2 gases.

The third experimental sample, (Fig. 3(c)) was used to study coupled SPPs as a means of increasing emission efficiency. This sample (Fig. 3(c)), contained a 43 ± 2 nm thick microstructured metal film (λ_g = 338 ± 1 nm) constructed in an identical manner to that used in the sample shown in Fig. 3(b). However, the emissive Alq_3 layer differed from that used in the previous samples being deposited by means of spin coating rather than evaporation. This was achieved by doping a polymer, polymethylmethacrylate (PMMA), with Alq_3 (3% by weight). The substrate was then coated with the PMMA/Alq_3 solution and spun at a rate of 4000 rpm, the thickness of the resulting film was found to be ~ 160 nm. To couple the modes associated with each interface of the metal together a dielectric overlayer of an appropriate thickness was added to the metal/air interface. This dielectric overlayer was formed using monolayers of the material 22-tricsenoic acid (22-tric) deposited onto the metal film using the Langmuir-Blodgett (LB) technique [15]. This technique allowed the thickness of the dielectric overlayer to be built up with nanometer precision thus providing great control over the effective refractive index at the metal/ dielectric overlayer-air boundary.

#4590 - $15.00 US Received 10 June 2004; Revised 29 June 2004; accepted 30 June 2004

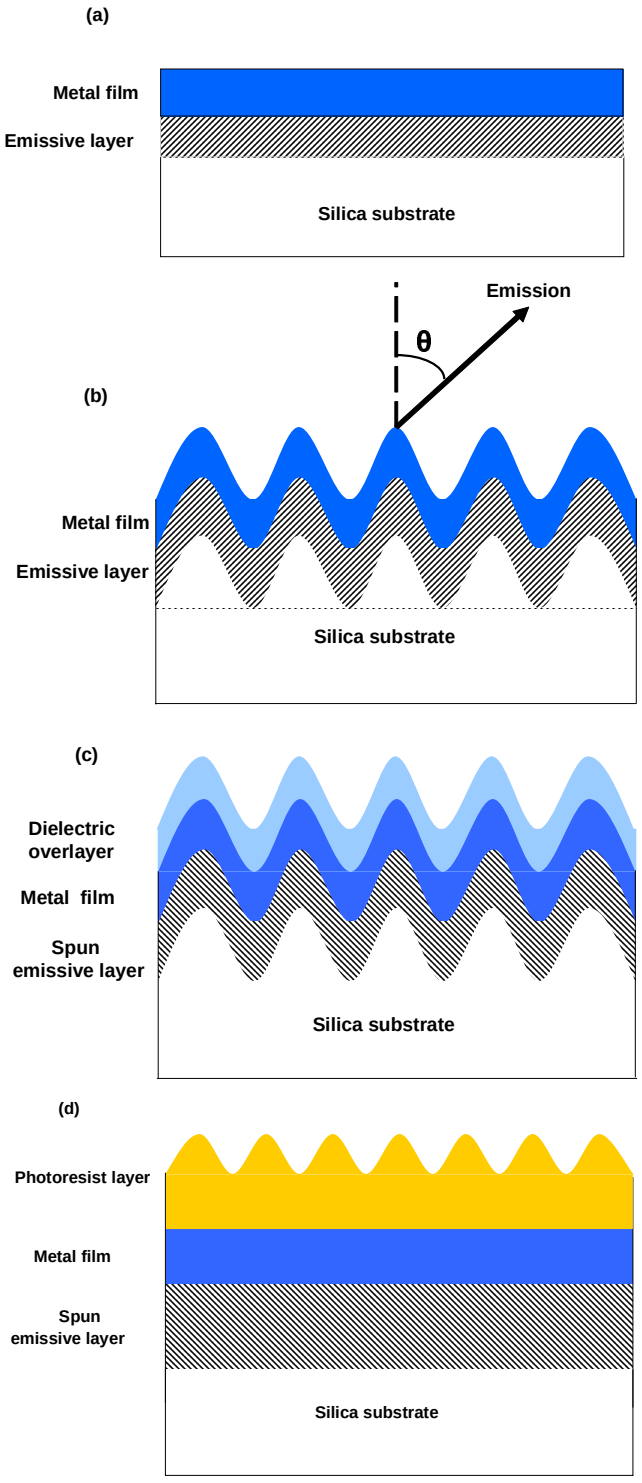

Fig. 3. Schematic representations of the experimental structures used in this study. (a) A 60 nm thick evaporated Alq_3 layer coated with a 55 nm thick planar silver film. (b) A 60 nm thick evaporated Alq_3 layer coated with a microstructured (λ_g = 338 nm) 55 nm thick silver film. (c) A 43 nm thick microstructured (λ_g = 338 nm) silver film bounded on one side by a 160 nm thick spun Alq_3 film and on the other by a dielectric overlayer (22-tric). (d) A 55 nm thick planar silver film bounded on one side by a 160 nm spun Alq_3 layer and on the other by a ~ 100 nm thick microstructured (λ_g = 485 mn) photoresist overlayer.

#4590 - $15.00 US
Received 10 June 2004; Revised 29 June 2004; accepted 30 June 2004

The final structure, (Fig. 3(d)) consisted of a 55 ± 2 nm thick planar silver film bound on one side by a ~160 nm thick spun Alq_3 layer. The other side of the Ag was spin coated with a PR film, into this film a microstructure was introduced (period λ_g = 485 nm) using the holographic technique detailed above, the thickness of this microstructured PR film was ~100 nm. The microstructured PR film served two purposes. Firstly, the thickness of the PR film was such that the effective refractive index of this layer was matched to the index of the emissive layer, thus allowing the SPP modes associated with each metal/dielectric interface to couple. Secondly, the microstructure contained within the PR enabled the coupled SPPs modes to scatter to light. The purpose here was to show if energy might be transported across a thin metal film via coupled SPPs and these modes scattered to light by utilizing a sample geometry that was easier to fabricate than a structure containing a microstructured metal film.

The construction of 4 different sample geometries enabled the transfer of energy across a thin metal film mediated by both cross-coupled and coupled SPPs to be investigated by measuring the photoluminescence (PL) emission from each structure.

3. Experimental technique

To measure the angle dependent PL, samples were mounted on a rotation stage and the Alq_3 optically pumped through the silica substrate with light from a 410 nm diode laser. The spectrum of the resulting PL emitted through the silver film was recorded using a spectrometer/CCD combination with a spectral resolution of ~ 2 nm, having first been passed through a narrow aperture to limit the collection angle to 1˚. By rotating the sample whilst keeping the collection optics stationary, emission spectra could be recorded for a range of polar emission angles (θ). In order to keep the optical pumping conditions constant the angle of the pump beam relative to the sample was fixed throughout each experiment.

4. Results

Figure 4 shows PL emission spectra measured at a polar emission angle, θ, of 10˚ from each of the structures shown in Fig. 3, these spectra were collected with a polarizer set to pass TM polarized light in front of the detector. It should be noted that each of these spectra have been normalized with respect to the emission from the planar control sample (Fig 3. (a)). From Fig. 4 it may be seen that each of the spectra obtained from the samples containing microstructure feature sharp emission peaks, these features are mediated by SPP modes supported by the structures being Bragg scattered to light from the microstructure. Considering the relative intensity of the PL emission from each of the structures, the peak emission from the samples that support coupled SPP (Figs. 3(c) and 3(d)) is greater than that from the cross-coupled sample shown in Fig. 3b by an order of magnitude, and are approximately 50 times greater than that from the planar sample (Fig. 3(a)). In order to investigate if these results were repeated over a range of emission angles the measured spectra obtained from each of the structures were built up to form dispersion maps. These maps were constructed by converting the data from PL intensity as a function of both emission angle and wavelength to intensity as a function of both in-plane wavevector and angular frequency.

#4590 - $15.00 US Received 10 June 2004; Revised 29 June 2004; accepted 30 June 2004

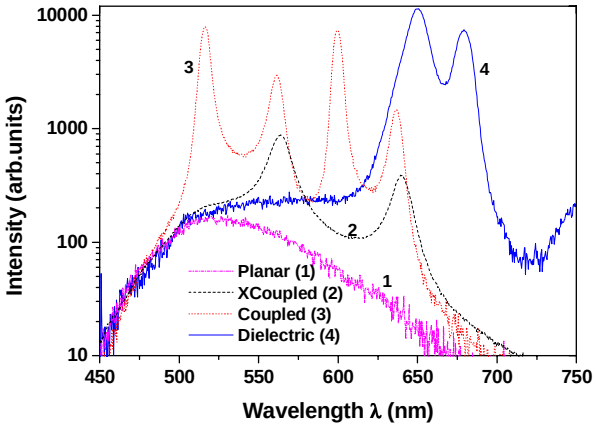

Fig. 4 TM polarized photoluminescence emission spectra measured through the metal film from each of the structures shown in Figure 3. Each spectrum was measured at a polar emission angle θ of 10˚. Note each spectrum has been normalized with respect to the emission spectrum obtained from the structure shown in Fig. 3a. This normalization was achieved by fitting the spectra obtained from the 3 microstructured samples to the spectrum obtain from the planar structure over a wavelength range from 400nm to 480 nm.

Figure 5 shows the dispersion maps constructed from TM polarized PL data obtained from the structures shown in Figs. 3(b), 3(c) and 3(d), with light regions representing areas of strong emission. The dispersion map constructed from data measured from the structure containing a microstructured metal film but no dielectric overlayer (Fig. 5(a)) shows a number of emission features. These emission maxima are mediated via the SPPs associated with both the Ag/organic and Ag/air interfaces and will be referred to as SPP1 and SPP2 respectively. Comparing these data (Fig. 5(a)) with the schematic dispersion map shown in Fig. 1(b) it may be seen how the scattering of the SPP modes from the microstructured metal film enables the SPPs to fall within the light cone and therefore couple to light. It should be noted that the region where SPP1 and SPP2 cross ($k_{//} \sim 0.87\ (\mu m)^{-1}$, $\omega \sim 1.98\ (\mu m)^{-1}$) has been overexposed in order that the emission mediated via the individual SPP modes may be seen more clearly. Note how weak emission mediated via SPP2 is in contrast to the amount of power lost to this mode, dramatically illustrating the effect of destructive interference between the two emission pathways for this mode, as noted above. Emission at the crossing of these two SPP modes is mediated via cross-coupling across the metal when Eq. (1) and (2) are met. As we have recently shown, emission via cross-coupled SPPs may result in a doubling of the PL intensity over the PL mediated via the sum of the individual two modes [16]. However, from Fig. 5(a) it is clear that SPP cross-coupling occurs only over a narrow range of emission wavelength and angles. Such a cross-coupling scheme may therefore not be best suited to applications such as displays. As noted above the peak emission of the PL spectra measured at an emission angle θ of 10° (Fig. 4) from a structure that supports coupled SPPs was an order of magnitude greater than from the structure shown in Fig. 3(b). To investigate if this increase in emission was repeated over a range of emission angles the PL from the structure shown in Fig. 3(c) was examined in greater detail.

#4590 - $15.00 US
Received 10 June 2004; Revised 29 June 2004; accepted 30 June 2004

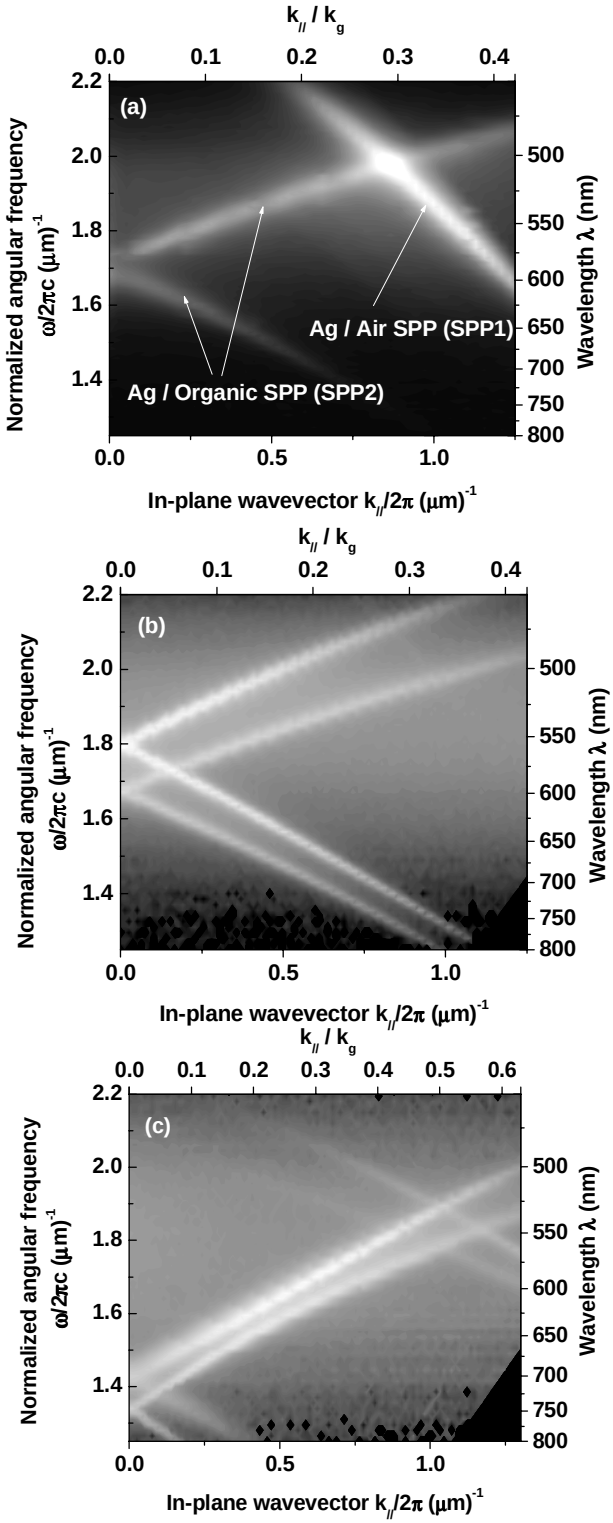

Fig. 5. Dispersion maps of the TM polarized photoluminescence emission obtained from the structures shown in (a) Fig. 3b, (b) Fig. 3c and (c) Fig. 3d. Light regions indicate areas of strong emission. Note, in Fig. 5a, in order to see the modal features more clearly the intensity at the crossing point between the Ag/organic SPP (SPP2) and the Ag/air SPP (SPP1) is overexposed.

#4590 - $15.00 US Received 10 June 2004; Revised 29 June 2004; accepted 30 June 2004

Figure 5(b) shows the dispersion map constructed from the PL emission measured from the sample shown in Fig. 3(c) with a dielectric overlayer thickness of 156.0 nm. These data show strong emission from a pair features across a range of emission angles and wavelengths. Comparing Figs. 5(a) and 5(b) it may be seen that the lower emission feature (Fig. 5(b)) corresponds to SPP2 seen in Fig. 5(a). The upper emission feature in Fig. 5(b) corresponds to SPP1 (Fig. 5(a)). The addition of the dielectric overlayer has caused the Ag/air SPP (SPP1) to downshift in frequency due to the increase in the effective refractive index at this interface. Strictly it is incorrect to refer to the SPP modes as being associated with either of the metal dielectric interfaces in a structure that supports coupled modes, rather they are symmetric and antisymmetric coupled surface plasmon polaritons [17].

To gain an understanding of how the addition of a dielectric overlayer to a thin metal might affect the coupling between the emissive layer and the modes supported by the structure further numerical modeling was undertaken [6]. These data (Fig. 6) were obtained by calculating the power dissipated by an emissive source located in Alq_3/PMMA film, as a function of dielectric overlayer thickness and in-plane wavevector. For a bare metal film the emitter may be seen to strongly couple to SPP2, in contrast SPP1 is not visible. These data are the same as those seen in Fig. 2 and show that the coupling between the emitter and the Ag/organic SPP (SPP2) being approximately 100 times stronger than to the Ag/air SPP (SPP1). Figure 6 shows that the addition to the metal of a dielectric overlayer ~ 50 nm thick results in an increase in power dissipated to SPP2. As the dielectric overlayer is further increased the power dissipated to SPP1 continues to rise whilst the coupling between the emitter and SPP2 may be seen to fall. The power coupled to SPP1 reaches a maximum for a dielectric overlayer thickness of ~ 150 nm. This increase in power between the emitter and the SPP associated with the Ag/air interface illustrates how matching the effective refractive indices of the media bounding a thin metal film may facilitate transport of energy across the film. From Fig. 6 it would appear that this transfer of energy is at a maximum for a dielectric overlayer thickness of ~ 150 nm. To see if this transfer of energy was accompanied by a corresponding increase in emission the PL from samples with a range of dielectric overlayer thicknesses were measured.

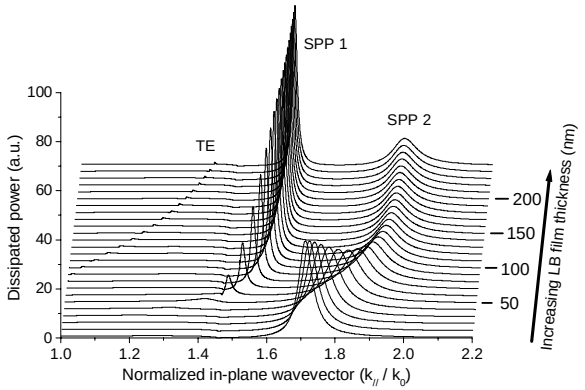

Fig. 6. Theoretically derived dispersion data showing the power dissipated from a dipole source to modes supported by the a metal film bounded on one surface by a spun Alq_3 film and on the other by an 22-tric dielectric overlayer, as a function of dielectric overlayer thickness and in-plane wavevector. For a structure with no dielectric overlayer SPP1 and SPP2 correspond to the SPP modes associated with the metal/air and metal/organic interfaces respectively. TE corresponds to a TE polarized waveguide mode supported by the system.

In order to examine the relative PL intensity emitted through a thin metal film between structures supporting individual and coupled SPP modes, samples with 9 different dielectric overlayer thicknesses were measured, the dielectric ranging from 0 to 197.6 nm in thickness.

#4590 - $15.00 US Received 10 June 2004; Revised 29 June 2004; accepted 30 June 2004

To compare the relative emission from each region the spectra obtained for a range of polar angles from 0 to 40˚ in one degree intervals were summed together. This summed intensity was then plotted as a function of wavelength. The area under each of these curves, over a wavelength range from 416 nm to 806 nm, was then determined by integration.

Figure 7 shows the integrated emission intensity for both TM and TE polarized emission as a function of dielectric overlayer thickness. Also shown is the integrated TM polarized emission intensity from the planar control sample (Fig. 3(a)). It may be seen from Fig. 7 that for relatively thin overlayers (26.0 nm to 67.6 nm) the intensity of the TM polarized PL is the same as that from the corrugated sample with no overlayer, i.e. a bare metal film (to within experimental error). For dielectric film thicknesses greater than ~ 75 nm the PL emission intensity is seen to increase sharply. As further dielectric overlayers are added the integrated emission intensity continues to increase until a maximum is reached when the SPP modes supported by the structure are best coupled, for a dielectric overlayer thickness of 156.0 nm. For dielectric overlayer thicknesses greater than this, i.e. 176.0 nm and 197.6 nm, the integrated emission intensity falls.

To ensure that the fall in the emission intensity seen from structures with a dielectric overlayer thickness of greater than 156.0 nm was not due to power from the emitter being lost to guided modes in the dielectric film, measurements were also taken of the TE polarized emission. For samples with a dielectric overlayer thickness greater than 100 nm, a peak in the TE polarized emission corresponding to a guided mode was seen. This TE polarized PL emission data was summed and integrated in the same manner as the TM polarized data. From Fig. 7 no increase may be seen in the TE polarized emission with increasing dielectric film thickness. These results show that the fall in the TM polarized emission intensity from the structures with dielectric overlayer thicknesses of 176.8 nm and 197.6 nm is due to a decrease in the coupling of the SPP modes rather than due to a redistribution of the power from the SPP modes to TE guided modes.

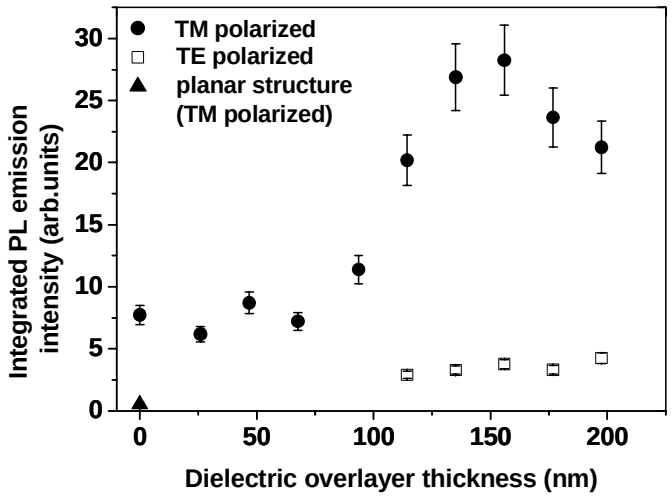

Fig. 7. Integrated intensity of PL emission obtained from the structure seen in Fig. 3b as a function of dielectric overlayer thickness. Also shown is the integrated TM polarized PL emission intensity from the structure shown in Fig. 3a. (Note for dielectric overlayer thicknesses below 114.4 nm no TE polarized emission features were seen).

The strength of integrated PL emission from a corrugated structure that supports coupled SPPs may be seen from these data to be 3 times greater than a similar sample with a bare corrugated metal film, and over 50 times greater than from a bare planar structure. Whilst the use of a sample containing a microstructured thin metal film that supports coupled SPPs has been shown to considerably increase the PL emission over a planar structure, the production

#4590 - $15.00 US Received 10 June 2004; Revised 29 June 2004; accepted 30 June 2004

of a microstructured metal film on a commercial scale is demanding in terms of fabrication. For this reason a sample was constructed that contained a planar metal film coated with a microstructured PR layer. This PR layer both allowed the SPPs associated with either side of the metal to couple and for the coupled SPPs to scatter to light.

Figure 5(c) shows a dispersion map constructed from the PL emission measured from the structure with a planar metal film and a microstructured PR layer (Fig. 3(c)). From these data a pair of emission features mediated via coupled SPPs similar to those shown in Fig. 5(b) may be seen. It should be noted that the difference in the position between the features seen in Figures 5(b) and 5(c) are due to the difference in grating pitch between the two structures. As with the previous sample (Fig. 3(c)) the PL emission through the metal film mediated via coupled SPPs may be seen to occur over a range of emission wavelengths and angles. This emission is remarkable considering the distance (~ 150 nm) between the emissive Alq_3 layer and the scattering surface located at the PR/air interface. Such an approach, where a wavelength scale microstructured dielectric overlayer is added to a cathode emitting OLED possibly by means of solvent assisted lithography, may open a practical way to increase device efficiency.

5. Conclusions

It has been shown that losses to surface plasmon-polariton (SPP) modes supported by a cathode emitting OLED may considerably diminish the efficiency of light emitting structures; the majority of this energy being lost to the SPP mode associated with metal/organic interface. Whilst some energy may be recovered by the introduction of a wavelength scale microstructure to the metallic cathode, thereby scattering the SPPs to light [18-19], much of this energy is lost due to both attenuation incurred in crossing the metal film and phase cancellations. We have shown that these losses may in part be overcome by selecting a sample geometry that allows the SPP modes associated with either side of a thin metal film to couple, thus enabling energy to be transported across the metal. One such method is SPP cross-coupling, PL emission mediated via this route has been shown to be two times greater than from the sum of the emission from the individual SPP modes. However, the emission mediated by cross-coupled SPPs has been shown to occur only over a narrow range of emission wavelength and angles.

An alternative means to recover energy lost to SPP modes has been presented where the SPP modes associated with either side of a thin metal film are coupled together across a wide range of emission frequencies by the addition onto the metal film of an appropriate dielectric overlayer. Two such schemes have been considered here, the first of these utilizes a microstructured metal film to scatter the coupled SPPs to light. The PL emission from such a structure has been shown to be 3 times greater than from a corrugated sample with a bare metal film and over 50 times greater than from a bare planar film. PL emission has also presented from a structure containing a planar metal film with the scattering surface being introduced into the dielectric overlayer, thus simplifying device fabrication. Strong PL emission from this structure mediated via coupled SPPs has been shown to occur across a range of emission angles and wavelengths. Such a device, in which a microstructured dielectric overlayer might be added to an OLED structure, possibly by means of soft lithography [20], may open possibility of increasing the optical out-coupling and thus the efficiency of devices such as top-emitting OLEDs.

Acknowledgments

This work was supported by the Materials Domain of the UK MoD Corporate Research Program and partly funded by the United Kingdom EPSRC. The partial support of this work by the EC funded project “Surface Plasmon Photonics” NMP4-CT-2003-505699 is also gratefully acknowledged.

#4590 - $15.00 US Received 10 June 2004; Revised 29 June 2004; accepted 30 June 2004